

# Development and validation of a high-throughput LC–MS/MS assay for routine measurement of molecular ceramides

Dimple Kauhanen<sup>1</sup> · Marko Sysi-Aho<sup>1</sup> · Kaisa M. Koistinen<sup>1</sup> · Reijo Laaksonen<sup>1</sup> · Juha Sinisalo<sup>2</sup> · Kim Ekroos<sup>1</sup>

Received: 10 December 2015 / Revised: 9 February 2016 / Accepted: 15 February 2016 / Published online: 27 February 2016  
© Springer-Verlag Berlin Heidelberg 2016

**Abstract** Monitoring the levels of the ceramides (Cer) d18:1/16:0, Cer d18:1/18:0, Cer d18:1/24:0, and Cer d18:1/24:1 and ratios thereof in human plasma empowers the prediction of fatal outcome of coronary artery disease (CAD). We describe a validated liquid chromatography–tandem mass spectrometry (LC–MS/MS) methodology for clinical-scaled measurement of the four distinct ceramides. Rapid plasma precipitation was accomplished in 96-well format. Excellent extraction recoveries in the range of 98–109 % were achieved for each ceramide. Addition of corresponding D<sub>7</sub>-labeled ceramide standards facilitated precise quantification of each plasma ceramide species utilizing a novel short 5-min LC–MS/MS method. Neither matrix interference nor carryover was observed. Robust intra- and inter-assay accuracy and precision <15 % at five different concentrations were obtained. Linear calibration lines with regressions,  $R^2 > 0.99$ , were achieved for all analytes. Short-term bench top, long-term plasma, and extract stability demonstrated that the distinct ceramides were stable in the conditions evaluated. The validity of the methodology was demonstrated by determining the precise ceramide concentrations in a small CAD case–control study. Thus, our LC–MS/MS methodology features simple sample preparation and short analysis time for accurate quantification of Cer d18:1/

16:0, Cer d18:1/18:0, Cer d18:1/24:0, and Cer d18:1/24:1, designed for routine analysis.

**Keywords** Mass spectrometry · Chromatography · Ceramides · Cardiovascular · Clinical · High throughput

## Introduction

Ceramides have been implicated in mediating or regulating numerous central cellular processes such as proliferation, differentiation and senescence, stress responses, apoptosis, and inflammation. Harmful stimuli can activate these bioactive signaling lipids leading to numerous pathophysiological states including inflammatory diseases such as obesity and metabolic disorders [1]. We have identified four distinct molecular ceramides to be closely linked to cardiovascular disease [2]. Recently, we have shown that these ceramides are prominent markers in stratifying a patient's risk for fatal outcome of coronary artery disease (CAD) (Laaksonen R et al., submitted).

The de novo biosynthesis of ceramides, belonging to the category of sphingolipids, originates with the condensation of serine and palmitoyl-CoA, followed by reduction of the formed 3-keto sphinganine to produce sphinganine that serves as a primary building block of sphingolipids [3]. This long chain base (LCB), typically a linear 18 carbon alkane or alkene that contains a 1,3-dihydroxy-2-amino functional group, is further *N*-acylated with a wide variety of acyl-CoAs by a reaction that is catalyzed by a group of six enzymes: the ceramide synthases 1–6 [4]. Subsequently, dihydroceramide is formed, which by desaturation at the  $\Delta 4$  position is made into ceramide. Since numerous different LCBs, owing to carbon length, position, and number of double bonds, hydroxylations, or branching, and fatty acids varying in chain length of typically C14–C26 exist, a vast repertoire of molecular ceramide

**Electronic supplementary material** The online version of this article (doi:10.1007/s00216-016-9425-z) contains supplementary material, which is available to authorized users.

✉ Kim Ekroos  
kim.ekroos@zora.fi

<sup>1</sup> Zora Biosciences, Biologinkuja 1, 02150 Espoo, Finland

<sup>2</sup> Heart and Lung Center, Helsinki University Hospital, 00029 HUS Helsinki, Finland

species can be produced [5]. Ceramides can also be produced through breakdown of more complex sphingolipids, such as hydrolysis of sphingomyelins by sphingomyelinase and of glucosylceramides by glucosylceramidase [5].

In CAD subjects, the fatal outcome correlates with increased plasma levels of *N*-palmitoyl-D-erythro-sphingosine (Cer d18:1/16:0), *N*-stearoyl-D-erythro-sphingosine (Cer d18:1/18:0), and *N*-nervonoyl-D-erythro-sphingosine (Cer d18:1/24:1) and decreased levels of *N*-lignoceroyl-D-erythro-sphingosine (Cer d18:1/24:0). Especially, when used as ratios, they are significant predictors of cardiovascular death [2]. Numerous analytical methodologies have been established for the measurement of ceramides, including thin-layer chromatography [6], normal phase liquid chromatography [7], immunochemical methodologies [8], gas chromatography [9], and tandem mass spectrometry [10]. Yet, common drawbacks of most of these approaches have been their inability to resolve ceramides at the molecular species level and lack of sensitivity and throughput. These hurdles have been resolved in the recent evolution of mass spectrometry-driven lipid analysis, facilitating rapid and sensitive monitoring of molecular species either by shotgun lipidomics [11–13] or LC-based targeted lipidomics [14, 15]. Although these methodologies have not in general been designed for clinical routine use, this technology has been utilized to establish clinically relevant applications as for instance the measurement of Cer d18:1/22:0 and Cer d18:1/24:0 [16].

In this study, we developed and validated, according to the Food and Drug Administration (FDA) bioanalytical method validation guidance [17], a clinical-scaled high-throughput methodology that uses LC–MS/MS to simultaneously quantify Cer d18:1/16:0, Cer d18:1/18:0, Cer d18:1/24:0, and Cer d18:1/24:1 in human plasma. To gain increased throughput, and simultaneously controlling for the hazard of organic solvents, we supplemented this with a rapid precipitation procedure based on less hazardous organic solvents. This method was applied to accurately determine the plasma concentrations of the four selected ceramides and ratios thereof in a small CAD case–control study.

## Materials and methods

### Chemicals

*N*-Palmitoyl-D-erythro-sphingosine (Cer d18:1/16:0), *N*-stearoyl-D-erythro-sphingosine (Cer d18:1/18:0), *N*-lignoceroyl-D-erythro-sphingosine (Cer d18:1/24:0), *N*-nervonoyl-D-erythro-sphingosine (Cer d18:1/24:1), *N*-palmitoyl-D-erythro-sphingosine-d7 (D<sub>7</sub>-Cer d18:1/16:0), *N*-stearoyl-D-erythro-sphingosine-d7 (D<sub>7</sub>-Cer d18:1/18:0), *N*-lignoceroyl-D-erythro-sphingosine-d7 (D<sub>7</sub>-Cer d18:1/24:0), and *N*-nervonoyl-D-erythro-sphingosine-d7 (D<sub>7</sub>-Cer d18:1/

24:1) were purchased from Avanti Polar Lipids, Inc. (Alabaster, AL). Acquity BEH C18, 1.7 μm VanGuard Pre-Column, and Acquity BEH C18, 2.1 × 50 mm id. 1.7 μm were from Waters (Milford, MA). Methanol, ethyl acetate, 2-propanol, ultrapure water, ammonium acetate, acetonitrile (all LC–MS grade), and 5 % bovine serum albumin (BSA) were purchased from Sigma-Aldrich GmbH (Steinheim, Germany). Fresh human plasma from three healthy volunteers were donated to Zora. Fresh frozen pooled plasma (FFP) was purchased from Finnish Red Cross Blood Service. Plasma samples from the Corogene cohort [18] were obtained from Helsinki University Central Hospital. The Corogene study was approved by the medical ethics committee (University Central Hospital of Helsinki) and performed in accordance with the criteria described in the Declaration of Helsinki. Written informed consent was obtained from all patients.

### Sample preparation

All stock solutions (500 pmol/μl) were prepared in methanol. Working solution for calibration line and spiking in solution containing Cer d18:1/16:0, Cer d18:1/18:0, Cer d18:1/24:0, and Cer d18:1/24:1 was prepared by serial dilution. Internal standard (IS) solution containing D<sub>7</sub>-Cer d18:1/16:0 (0.125 pmol/μl), D<sub>7</sub>-Cer d18:1/18:0 (0.05 pmol/μl), D<sub>7</sub>-Cer d18:1/24:0 (1.5 pmol/μl), and D<sub>7</sub>-Cer d18:1/24:1 (0.5 pmol/μl) was prepared in methanol. Plasma was thawed at 4 °C and then brought to room temperature prior to extraction. An aliquot of standards, quality control (QC), matrix blank (10 μl), or study samples (10 μl) was transferred into 96-well (2 ml/well) plate. IS mixture (20 μl) was added followed by protein precipitation (PPT) solvent, ethyl acetate:isopropanol (2:8, v/v) to a final volume of 600 μl per sample. Samples were mixed for 10 min followed by centrifugation for 10 min at 3000×g force. The supernatant was then transferred to an Eppendorf twin.tec PCR Plate 96-well plate and sealed with a heatsealing foil (Hamburg, Germany) prior to analysis by LC–MS/MS.

### LC–MS/MS analysis

LC–MS/MS analysis was conducted on a SCIEX QTRAP® 6500 mass spectrometer coupled to an Eksigent ultraLC 110 system (Concord, Canada). Electrospray ionization (ESI) in positive ion mode using MRM was performed. The instrument and data acquisition was controlled using Analyst® 1.6.2. Prior to the validation work, compound optimization was assessed to obtain the optimal mass spectrometer conditions for analysis of Cer d18:1/16:0, D<sub>7</sub>-Cer d18:1/16:0, Cer d18:1/18:0, D<sub>7</sub>-Cer d18:1/18:0, Cer d18:1/24:0, D<sub>7</sub>-Cer d18:1/24:0, Cer d18:1/24:1, and D<sub>7</sub>-Cer d18:1/24:1. This was conducted by individually infusing the ceramide standards at 1 pmol/μl concentration at 20 μl/min. The following

settings were selected: curtain gas, 25 psi; ion spray voltage, 5000 V; temperature, 300 °C; gas 1 and gas 2, 50 and 30 psi, respectively; declustering potential, 30 V; entrance potential, 10 V; collision cell exit potential, 20 V; and collision energy, 40 eV. Chromatographic separation was performed on an Acquity BEH C18, 2.1 × 50 mm id. 1.7 μm column with a 1.7 μm VanGuard Pre-Column in front. The temperature was set at 60 °C. Mobile phases consisted of (A) 10 mM ammonium acetate in LC–MS grade water with 0.1 % formic acid and (B) 10 mM ammonium acetate in acetonitrile:2-propanol (4:3, v/v) with 0.1 % formic acid. Injection volume was 5 μl and the flow rate set to 500 μl/min. The following gradient was applied: A/B (15/85 %) from 0 to 0.5 min, then B to 100 % from 0.5 to 1.5 min, then B held at 100 % from 1.5 to 4.0 min, and finally changed to A/B (15/85 %) from 4.0 to 5.0 min.

### Calibration curves

Due to the presence of endogenous lipids in human plasma and unavailability of lipid-free plasma matrix, calibration line standards were prepared with 5 % BSA. Linearity of the assay was determined by decreasing the amount of each endogenous lipid in six steps. Final concentrations of the calibration line points for Cer d18:1/16:0 and Cer d18:1/18:0 included 0.008, 0.01, 0.02, 0.1, 1, and 2 pmol/μl and for Cer d18:1/24:0 and Cer d18:1/24:1 0.08, 0.1, 0.2, 1, 10, and 20 pmol/μl. A fixed amount of D<sub>7</sub>-internal standards were added to the calibration line standards followed by PPT solvent. BSA substituted with water was used as total blank and human plasma as matrix blank. In each assay, two calibration line sets were included containing all four analytes. All calibration curves were weighted by  $1/x^2$ , inverse of the squared concentration, to focus the calibration line to the lower points in the calibration line, hence reducing quantitation error at low concentrations. To address the parallelism of the calibration lines, standards prepared in 5 % BSA and plasma were evaluated. Calibration line made from extracted plasma samples was compared against a line made in 5 % BSA. Plasma was diluted two- and three-fold to obtain lower calibration points, undiluted plasma represented middle point, and plasma was extracted by doubling and tripling the plasma volume in extraction to represent the higher points of the calibration line. The estimated 95 % confidence intervals of slopes were overlapping for both lines indicating their parallelism.

### Extraction recovery

Recovery of the extraction method was determined for each analyte by adding in endogenous standards into crude human plasma, prior to extraction, elevating the nominal concentration by 0.10 and 0.25 pmol/μl for Cer d18:1/16:0 and Cer d18:1/18:0 and 1.0 and 2.5 pmol/μl for Cer d18:1/24:0 and

Cer d18:1/24:1. Extraction recovery was estimated from the increase in measured concentration after standard addition divided by the concentration that was added.

### Quality controls

FFP was used to represent QC samples. To establish the endogenous concentration of each ceramide, untreated FFP was extracted and analyzed in six replicates ( $n=6$ ). Untreated FFP represented middle quality control (MQC), low QC (LQC), and lower limit of quantification QC (LLOQ) were prepared by diluting MQC two- and three-fold with water. High QC (HQC) and upper limit of quantification QC (ULOQ) were prepared by spiking in endogenous standards. Internal standards were added to all QC samples and were bulk prepared and stored in separate aliquots at –80 °C prior to extraction.

### Intra- and inter-assay variation

The precision and accuracy of the assay was determined for each of the four ceramides at five different concentrations, LLOQ, LQC, MQC, HQC, and HLOQ. Intra-assay variation, precision, and accuracy was calculated for each of the ceramide in replicates of six ( $n=6$ ) at each QC concentration independently on three separate occasions. Inter-assay variation, precision, and accuracy was calculated from three ( $n=3$ ) intra-assay extractions that were analyzed on three separate occasions. The intra- and inter-assay precisions (percentage coefficient variance, %CV) and accuracies (percentage accuracy, %Accuracy) were calculated from the nominal concentrations.

### Stability of quality controls

Bench top stability at room temperature and at 4 °C, three freeze and thaw (F/T) cycles, extract stability on autosampler, and calibration line stability at –20 °C were determined for each of the analytes in HQC, LQC, and MQC. For bench top stability, QCs were kept at room temperature for 4 h and at 4 °C for 24 h prior to PPT extraction. For F/T stability, QCs were frozen overnight and thawed the following day. This process was repeated twice and on the third thaw cycle, QCs were extracted. Bench top and freeze thaw QC's ceramide levels were compared to their corresponding freshly extracted nominal concentrations. Autosampler stability was determined by analysis of freshly extracted QCs compared to the same QCs re-analyzed 44 h after stored in autosampler at 8 °C using a freshly prepared calibration line. Calibration line stability was assessed by analyzing calibration lines fresh against stored at –20 °C for 9 days.

For long-term storage stability assessment, human plasma ( $n=6$ ) was stored at –80 °C up to 80 days and compared to corresponding freshly extracted human plasma.

## Analysis of clinical samples

Corogene (NCT00417534) is a prospective, consecutive cohort study consisting of 5294 Finnish patients assigned to coronary angiogram in Helsinki University Central Hospital between 2006 and 2008. The study design including sample collection information has been described by Vaara et al. [18]. We analyzed plasma samples from 42 cases and 42 matched controls. The cases were CAD patients who had experienced a coronary death within an average follow-up of 2.5 years after a diagnostic angiogram, whereas the controls were stable CAD patients who remained alive during the follow-up period. Matching was based on age, sex, smoking, type 2 diabetes, and statin use at study entry. Study samples were extracted and analyzed as described in this article. Each assay included a calibration curve before and after study samples and MQC in replicates of six ( $n=6$ ).

## Statistical analysis

Wilcoxon's rank-sum test was applied to assess differences between the case and control groups. Calibration lines were estimated with the weighted least squares method with the weights being inversely proportional to the squares of the actual concentrations. Two or more calibration lines were considered parallel if their slopes were within the intersection of the 95 % confidence intervals of the slopes.

## Results

### LC-MS/MS assay development and validation

Previous work has demonstrated the analysis of ceramides by ESI-MS, including in-depth characterization of their fragment mechanisms [10, 19–21]. Under the applied ESI-MS conditions, Cer d18:1/16:0, Cer d18:1/18:0, Cer d18:1/24:0, and Cer d18:1/24:1 and their respective deuterated versions generate  $[M+H]^+$  ions. The product ion spectra of the protonated precursor ions showed the expected ceramide fragment ion profiles [10], producing the most abundant ion at  $m/z$  264.3, arising from loss of the fatty acyl (Fig. 1a). The deuterated ceramides provided similar product ion spectra, due to the deuterium-labeled LCB producing the expected 7 Da mass shift in the LCB containing product ions (Fig. 2b). Therefore, the most abundant product ion of the deuterated ceramides is expected at  $m/z$  271.3. We selected the product ion  $m/z$  264.3 for endogenous ceramides and  $m/z$  271.3 for the deuterated ceramides and performed compound optimization to provide the highest abundance of these characteristic ions. These product ions were selected together with their respective parent ions as the MRM pairs.

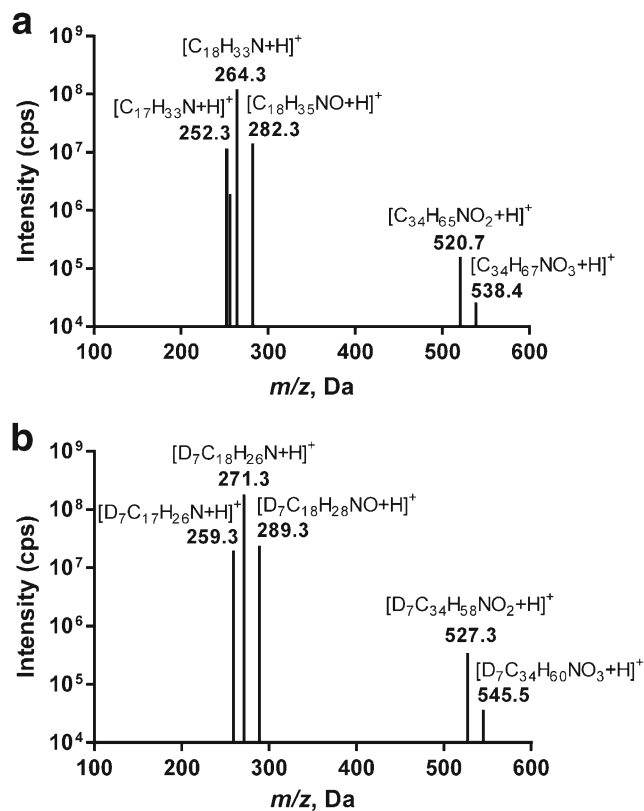


**Fig. 1** Representative product ion spectra of Cer d18:1/16:0 (a) and the corresponding deuterated standard D<sub>7</sub>-Cer d18:1/16:0 (b). The  $m/z$  and type of fragment ion are shown

The LC-MS/MS approach provided baseline separation of Cer d18:1/16:0, Cer d18:1/18:0, Cer d18:1/24:0, and Cer d18:1/24:1 (Fig. 2k–o). Performing enhanced product ion scanning on each ceramide peak in human plasma verified their correct identities and confirmed no overlap or interference of potential background ions. Thus, the chosen  $m/z$  MRM pairs, 538.5/264.3 for Cer d18:1/16:0, 566.5/264.3 for Cer d18:1/18:0, 650.5/264.3 for Cer d18:1/24:0, and 648.5/264.3 for Cer d18:1/24:1, facilitated highly selective monitoring of the ceramides of interest. We obtained analogous results with the D<sub>7</sub>-labeled ISs, producing background-free response signals of respective species by choosing the  $m/z$  transitions: 545.5/271.3 for D<sub>7</sub>-Cer d18:1/16:0, 573.5/271.3 for D<sub>7</sub>-Cer d18:1/18:0, 657.5/271.3 for D<sub>7</sub>-Cer d18:1/24:0, and 655.5/271.3 for D<sub>7</sub>-Cer d18:1/24:1 (Fig. 2p–t). Monitoring MQCs showed that the intensities of the deuterated standards were almost identical to the respective endogenous species. None of the analytes were detected in total blank (Fig. 2a–e). Moreover, no signals of the respective deuterated compounds were observed in matrix blank, LLOQ, extracted FFP, and human plasma, showing no interference coming from the IS and that no matrix effect was observed from plasma in the IS transitions. The retention time of respective endogenous species matched precisely the deuterated standards, further verifying the correct identity of each lipid. Finally, no carryover

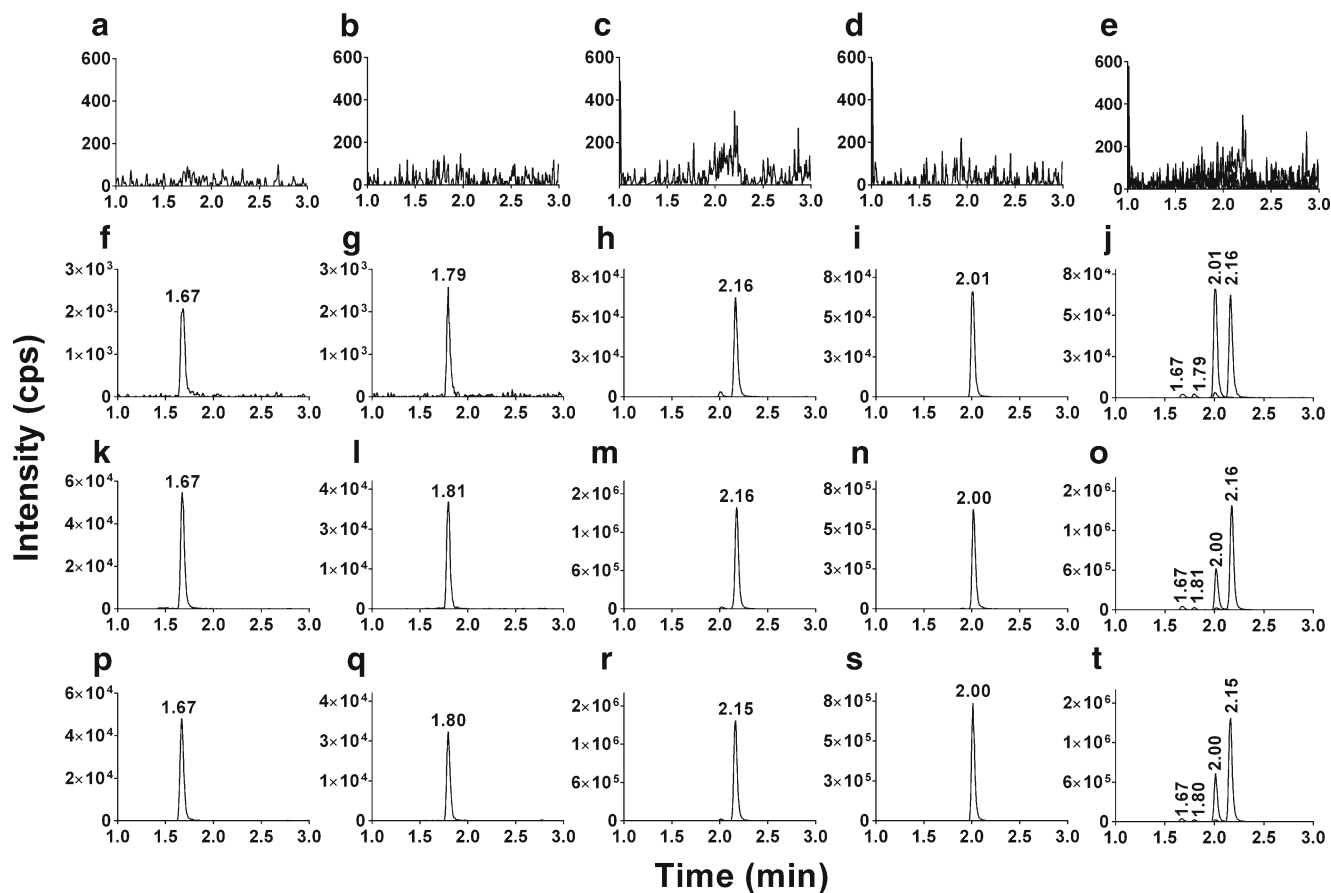


**Fig. 2** LC-MRM chromatograms of total blank (a–e), LLOQ (f–j), and MQC (k–o) for Cer d18:1/16:0, Cer d18:1/18:0, Cer d18:1/24:0, and Cer d18:1/24:1 and their overlaid chromatograms. LC-MRM chromatograms

of MQC (p–t) for D<sub>7</sub>-Cer d18:1/16:0, D<sub>7</sub>-Cer d18:1/18:0, D<sub>7</sub>-Cer d18:1/24:0, and D<sub>7</sub>-Cer d18:1/24:1 and their overlaid chromatograms

effect was observed in any transitions monitored by analyzing the highest calibration curve standard and highest QC immediately followed by a blank solvent injection (not shown).

The calibration curves prepared in 5 % BSA and solution showed linearity for all four ceramides with coefficients of determination ( $R^2$ ) above 0.99 (Fig. 3). The linear range for Cer d18:1/16:0 and Cer d18:1/18:0 were 0.008 to 2 pmol/ $\mu$ l and 0.08 to 20 pmol/ $\mu$ l for Cer d18:1/24:0 and Cer d18:1/24:1. The signal-to-noise ratio of the lowest calibration line point was greater than 10 for all four ceramides, defined as LLOQ shown in Fig. 2f–j. We also determined parallelism of calibration lines prepared in 5 % BSA and human plasma. No significant differences in the slopes were obtained based on the fact that all determined slope estimates overlapped inside the 95 % confidence interval (not shown).

Assay recovery was determined by adding in endogenous standards into human plasma elevating the nominal concentration by 0.10 and 0.25 pmol/ $\mu$ l for Cer d18:1/16:0 and Cer d18:1/18:0 and 1.0 and 2.5 pmol/ $\mu$ l for Cer d18:1/24:0 and Cer d18:1/24:1. The obtained recoveries were in the range of 98 to 109 % for all four ceramides (see Electronic Supplementary Material (ESM) Table S1).

Intra- and inter-assay precisions and accuracies of the method were determined analyzing FFP over three consecutive runs (Table 1). Bulk prepared QCs at five different concentrations were analyzed. The obtained ceramide concentrations of the untreated QC (MQC) was set as nominal values and used for calculating the levels in LQC, LLOQ, HQC, and ULOQ. In this way, the final QC concentration ranged from 0.080 to 0.490 pmol/ $\mu$ l for Cer d18:1/16:0, 0.033 to 0.348 pmol/ $\mu$ l for Cer d18:1/18:0, 0.863 to 5.090 pmol/ $\mu$ l for Cer d18:1/24:0, and 0.294 to 3.383 pmol/ $\mu$ l for Cer d18:1/24:1. Intra-assay accuracy and CV for all of the four ceramides were <15 % covering all concentrations. The inter-assay accuracy ranged from –2.2 to 1.9 % for Cer d18:1/16:0, 4.2 to 9.9 % for Cer d18:1/18:0, 3.5 to 8.6 % for Cer d18:1/24:0, and 2.5 to 10.4 % for Cer d18:1/24:0 inside the measured concentration range. Similarly, inter-assay CV ranged from 5.1 to 11.8 % for all four ceramides.

The stability of Cer d18:1/16:0, Cer d18:1/18:0, Cer d18:1/24:0, and Cer d18:1/24:1 in FFP was evaluated under several different conditions. The accuracy of bench top stability monitored at room temperature for 4 h and at 4 °C for 24 h for LQC, MQC, and HQC, respectively, were in acceptable range,

**Fig. 3** Six-point calibration curves for Cer d18:1/16:0 (a), Cer d18:1/18:0 (b), Cer d18:1/24:0 (c), and Cer d18:1/24:1 (d) in 5 % BSA. A magnification of the four lowest concentrations is shown as an inset. Two independent calibration lines were analyzed consecutively. The linear regression line and the  $R^2$  were calculated from the mean of the two independent  $1/x^2$  weighted calibration lines

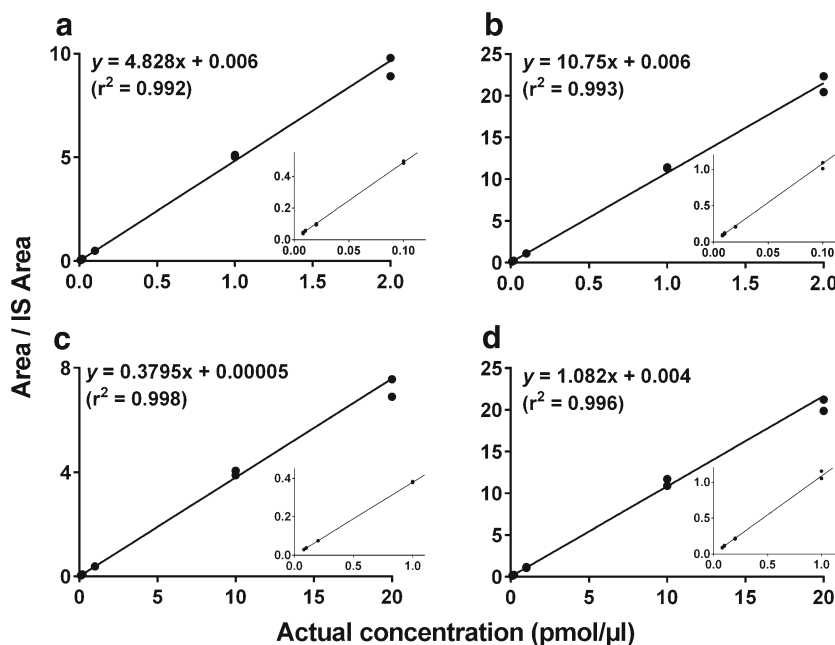


**Table 1** Precision and accuracy of LC–MS/MS for Cer d18:1/16:0, Cer d18:1/18:0, Cer d18:1/24:0, and Cer d18:1/24:1 analysis

		LLOQ	LQC <sup>a</sup>	MQC	HQC	ULOQ
Cer d18:1/16:0						
Nominal concentration, pmol/μl		0.08	0.12	0.24	0.34	0.49
Intra-assay	%Accuracy	3	−0.5	2.8	2.5	−1.4
	%CV	6.8	5.9	6.4	5.9	5.2
Inter-assay	%Accuracy	0.2	0.2	1.5	−2.2	1.9
	%CV	8.2	7	8.6	8.9	6.7
Cer d18:1/18:0						
Nominal concentration, pmol/μl		0.03	0.05	0.10	0.20	0.35
Intra-assay	%Accuracy	10.6	9.5	14.9	9.3	7.6
	%CV	8.2	6.5	6.9	4.2	5.3
Inter-assay	%Accuracy	5.5	8	9.9	4.2	8.2
	%CV	10.9	6.5	10.5	8.4	5.1
Cer d18:1/24:0						
Nominal concentration, pmol/μl		0.86	1.30	2.59	3.59	5.09
Intra-assay	%Accuracy	12.9	9.5	13.1	12.8	6.7
	%CV	5.7	5.0	6.0	6.3	5.0
Inter-assay	%Accuracy	5.6	7.1	8.6	3.5	5.4
	%CV	10.2	6.6	10.1	11.8	6.6
Cer d18:1/24:1						
Nominal concentration, pmol/μl		0.29	0.44	0.88	1.88	3.38
Intra-assay	%Accuracy	7.4	7.1	10.6	7.3	7.2
	%CV	5.1	4.5	6.8	3.7	3.5
Inter-assay	%Accuracy	2.5	4.1	5.2	3.2	10.4
	%CV	8.1	6.5	10	5.7	5.3

<sup>a</sup> Inter-assay,  $n = 16$

<15 %, for all four ceramides (Table 2). Similarly, the sampled extracts stored at 8 °C in autosampler for 44 h showed adequate stability. Long-term storage stability of human plasma at −80 °C up to 80 days showed acceptable accuracy and precision (see ESM Table S2). Finally, the effect of three independent F/T cycles showed no significant effect on the sample stability, based on analysis of three individual human plasma subjects (see ESM Table S3).

## Application

Cer d18:1/16:0, Cer d18:1/18:0, Cer d18:1/24:0, and Cer d18:1/24:1 were quantified in plasma from a subset of patients of the Corogene cohort, as described in “Materials and methods.” The median concentrations of Cer d18:1/16:0, Cer d18:1/18:0, Cer d18:1/24:0, and Cer d18:1/24:1 in the case group were 0.25, 0.12, 2.04, and 1.22 pmol/μl, respectively, whereas in the control group, the concentrations were 0.23, 0.10, 2.23, and 1.18 pmol/μl, respectively. These results show the same trends as in previous work [2] and ongoing studies (Laaksonen R et al., submitted), namely that in the case group representing high-risk CAD patients, the levels of Cer d18:1/16:0, Cer d18:1/18:0, and Cer d18:1/24:1 increase, whereas the level of Cer d18:1/24:0 decreases (Fig. 4). We note that in this analysis set, only the Cer d18:1/18:0 showed significant change; however, significant changes in the other ceramides are also observed when the number of samples increases (Laaksonen R et al., submitted). Accordingly, the group differences dramatically increase when the ceramides are plotted as ratios, providing the highly significant signatures Cer d18:1/16:0/Cer d18:1/24:0 and Cer d18:1/24:1/Cer d18:1/24:0 elevated in high-risk CAD patients.

**Table 2** Sample stability of Cer d18:1/16:0, Cer d18:1/18:0, Cer d18:1/24:0, and Cer d18:1/24:1

		Cer d18:1/16:0			Cer d18:1/18:0			Cer d18:1/24:0			Cer d18:1/24:1		
		LQC	MQC	HQC	LQC	MQC	HQC	LQC	MQC	HQC	LQC	MQC	HQC
Nominal concentration, pmol/μl		0.12	0.24	0.34	0.05	0.10	0.20	1.30	2.59	3.59	0.44	0.88	1.88
Bench top at RT for 4 h <sup>a</sup>	%Accuracy	4.2	3	−4.9	4.8	7.9	−3.5	12	11.8	−1.2	7.5	6.5	−5.1
	%CV	6.7	10.6	7.1	8.8	10.6	8.9	6.7	9.2	8.3	6.9	11.2	8
Bench top at 4 °C for 24 h <sup>a</sup>	%Accuracy	4.5	7.1	−2.4	11.2	14.1	4.5	15	14.7	6.9	9.1	8.3	2.9
	%CV	6.9	10.9	4.4	8.9	10.1	6	9.5	11.6	5.1	9.3	11.4	4.7
Autosampler extract stability <sup>b</sup>	%Accuracy	−0.9	4.2	2.9	9.7	14.7	14.1	9.1	14.3	11.3	5.5	9.6	9.3
	%CV	6	6	5.7	5.2	7.3	3.8	4.1	6.4	4.2	3.9	7.3	4.9

<sup>a</sup> QCs were kept at room temperature for 4 h and at 4 °C for 24 h prior to PPT extraction. The stability was determined by comparing the QC's ceramide levels to their corresponding freshly extracted nominal concentrations

<sup>b</sup> Autosampler stability was determined by analysis of freshly extracted QCs compared to the same QCs re-analyzed 44 h after stored in autosampler at 8 °C

## Discussion

We describe for the first time a high-throughput LC–MS/MS assay for the routine measurement of Cer d18:1/16:0, Cer d18:1/18:0, Cer d18:1/24:0, and Cer d18:1/24:1 in human plasma to be used in clinical practices. The assay is highly sensitive and requires a total analysis time per sample as short as 5 min.

Several methodologies exist for measuring ceramides [6–10, 22–24]. However, most of the assays have been designed for discovery work and not for clinical use. Consequently, such assays are typically short in selectivity, throughput, precision, and accuracy, therefore not fulfilling the clinical laboratory required specifications. To date, only Jiang et al. [16] have demonstrated a clinically relevant ceramide assay focusing on targeted measurement of Cer d18:1/22:0 and Cer d18:1/24:0. They successfully accomplished this using LC–MS/MS rather than utilizing an immunoassay-based approach that is of more preference in clinical laboratories. In line with their work, we successfully extended the measurement to four individual ceramide species based on LC–MS/MS. The prime advantage of LC–MS/MS lies in the power of the chromatographic separation in conjunction with precise monitoring by mass spectrometry, offering unambiguous detection of each monitored molecular ceramide. In contrast, we failed in distinguishing the four ceramides using a traditional immunoassay-based approach, suggesting that the epitopes of each individual ceramide are too similar. Krishnamurthy et al. [25] have shown that anti-ceramide antibody recognizes an arsenal of molecular ceramides only different in the fatty acid chain length. Consequently, this low selectivity of the available antibodies currently hinders the development of a clinically valid immunoassay method.

Previous work has demonstrated the advantages and feasibility of LC–MS/MS in the measurement of hydrophobic analytes in clinical laboratories [26–29]. Molecular ceramides can readily be distinguished by ESI-MS by monitoring the characteristic product ion  $m/z$  264.3 originating from the selective loss of the LCB undergone loss of two water molecules [10]. This product ion together with respective parent ions has been the basis for successful monitoring of individual ceramides by LC–MS [30–32] and by shotgun-based analyses [33, 34]. We chose the same ions to provide the best discrimination of the monitored molecular ceramides, allowing us to

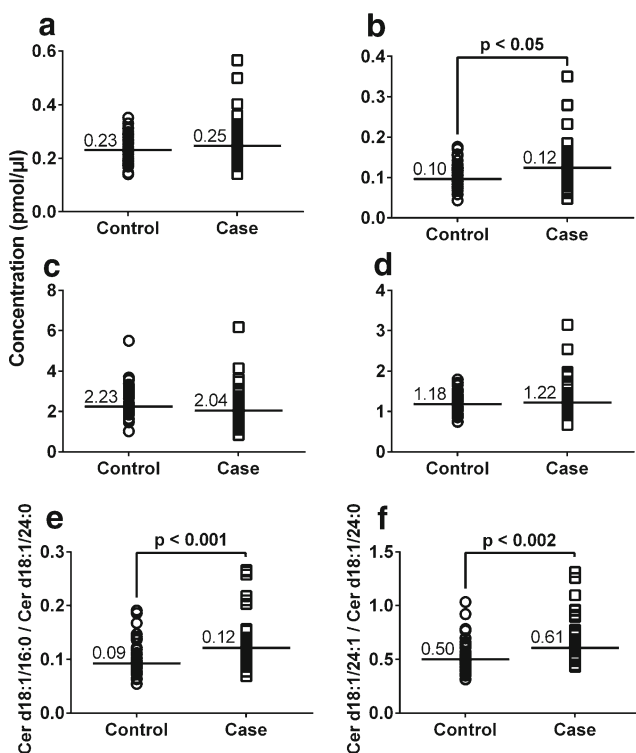


**Fig. 4** Concentration of Cer d18:1/16:0 (a), Cer d18:1/18:0 (b), Cer d18:1/24:0 (c), and Cer d18:1/24:1 (d) and ratio of Cer d18:1/16:0 to Cer d18:1/24:0 (e) and Cer d18:1/24:1 to Cer d18:1/24:0 (f) in controls and cases of the CAD study described in “Materials and methods.” The median concentrations (pmol/μl) and ratios are shown

reduce the chromatographic separation to 5 min without introducing any interference from co-eluting peaks and chemical noise in the monitored MRM transitions. The high selectivity is further mirrored in the MRMs of the deuterated standards by the insignificant background noise and, importantly, by the identical elution times as for the endogenous analytes. In our hands, the chosen MRM transitions gave the highest selectivity and also the best sensitivity, since the LCB-derived fragment ions gave the most intense signals.

Calibration lines generated from serial dilutions of the target analyte with fixed amount of the target standard are a common approach in bioanalysis to achieve precise and accurate quantification of the target analyte in the biological sample. It is preferred that the calibration line is prepared in sample matrix to best reflect the environment of the target analyte in the biological sample and, in this way, minimize potential negative effects of such ion suppression and extraction recovery leading to incorrect concentration estimates. However, a common hurdle in biomarker analysis is that an appropriate surrogate matrix has to be selected, since the sample matrix is typically not free of the target analyte. In our analysis, we found that 5 % BSA was an optimal substitute to human plasma, as this was also free of the ceramides. We obtained identical calibration lines in 5 % BSA and in human plasma, therefore proving the validity of using 5 % BSA as surrogate matrix.

The validated LC–MS/MS methodology allowed us to determine the precise levels of Cer d18:1/16:0, Cer d18:1/18:0, Cer d18:1/24:0, and Cer d18:1/24:1 in human plasma of 84 CAD patients. The concentration of Cer d18:1/24:0 in the control group is in good agreement with the measurements by Jiang et al. [16] who obtained a concentration of roughly 2.3 pmol/μl of the same ceramide in their control group. This verifies the validity of our approach, as the small concentration discrepancies are likely related to the phenotypical differences between the two control groups rather than any technical concerns. Thus, the obtained ceramide results from the current CAD study allow us to confirm our previous findings [2], showing that subjects at high risks of fatal outcome of CAD have higher levels of Cer d18:1/18:0. By increasing the study size will also provide significant changes in Cer d18:1/16:0, Cer d18:1/24:1, and Cer d18:1/24:0 with the two former increasing and the latter decreasing in cases compared to controls (Laaksonen R et al., submitted). However, significant group differences can already be observed in this small study size when the ceramides are plotted as ratios (Fig. 4).

## Conclusions and perspectives

We have developed and validated an LC–MS/MS assay for the routine analysis of four molecular ceramides. Its advantage is that it uses small sample volumes (10 μl) that are robustly

and rapidly prepared through a simple extraction procedure. The automated LC–MS/MS system allows up to 280 tests to be performed in a 24-h period. The method fulfills the validation criteria, set by FDA's bioanalytical method validation guideline [17], by showing good linearity and ≤15 % variation in recovery, accuracy, precision, and stability of each measured ceramide analyte. This method has been in routine use in our laboratory for more than 12 months, and >20,000 samples have successfully been analyzed. We expect that the number of analyses will exponentially increase over the next years. As a result, this will not only provide us with improved diagnosis of CAD subjects and understanding of the roles of the selected ceramides in cardiovascular disease but also deliver comprehensive information about the biological variation of the measured ceramides in larger populations covering different ethnical backgrounds. Expectedly, this paves the way in the establishment of valid reference values for these ceramides, benefitting disease areas and other settings where a precise assessment of these selected ceramides play pivotal roles. Taken together, we conclude that our developed assay is analytically valid and suitable for routine clinical and diagnostic use.

**Acknowledgments** We thank Walt Shaw and Lisa Connell at Avanti Polar Lipids for their great support. We thank all members of our laboratory for valuable discussions and suggestions. The research leading to these results has received funding from the European Union's Seventh Framework Programme FP7/2007-2013 under grant agreement no. 305739.

## Compliance with ethical standards

**Conflict of interest** The authors declare that there is no conflict of interest.

## References

1. Maceyka M, Spiegel S. Sphingolipid metabolites in inflammatory disease. *Nature*. 2014;510:58–67.
2. Tarasov K, Ekroos K, Suoniemi M, Kauhanen D, Sylvänne T, Humme R, et al. Molecular lipids identify cardiovascular risk and are efficiently lowered by simvastatin and PCSK9 deficiency. *J Clin Endocrinol Metab*. 2014;99:E45–52.
3. Haynes CA, Allegood JC, Park H, Sullards MC. Sphingolipidomics: methods for the comprehensive analysis of sphingolipids. *J Chromatogr B Analyt Technol Biomed Life Sci*. 2009;877:2696–708.
4. Mullen TD, Hannun YA, Obeid LM. Ceramide synthases at the centre of sphingolipid metabolism and biology. *Biochem J*. 2012;441:789–802.
5. Merrill AH. Sphingolipid and glycosphingolipid metabolic pathways in the era of sphingolipidomics. *Chem Rev*. 2011;111:6387–422.
6. Dobrzyń A, Górski J. Ceramides and sphingomyelins in skeletal muscles of the rat: content and composition. Effect of prolonged exercise. *Am J Physiol Endocrinol Metab*. 2002;282:E277–85.



7. Previati M, Bertolaso L, Tramarin M, Bertagnolo V, Capitani S. Low nanogram range quantitation of diglycerides and ceramide by high-performance liquid chromatography. *Anal Biochem.* 1996;233:108–14.
8. Vielhaber G, Brade L, Lindner B, Pfeiffer S, Wepf R, Hintze U, et al. Mouse anti-ceramide antiserum: a specific tool for the detection of endogenous ceramide. *Glycobiology.* 2001;11:451–7.
9. Samuelsson K, Sameulsson B. Gas chromatographic and mass spectrometric studies of synthetic and naturally occurring ceramides. *Chem Phys Lipids.* 1970;5:44–79.
10. Liebisch G, Drobnik W, Reil M, Trümbach B, Arnecke R, Olgemöller B, et al. Quantitative measurement of different ceramide species from crude cellular extracts by electrospray ionization tandem mass spectrometry (ESI-MS/MS). *J Lipid Res.* 1999;40:1539–46.
11. Simons B, Kauhanen D, Sylvänne T, Tarasov K, Duchoslav E, Ekroos K. Shotgun lipidomics by sequential precursor ion fragmentation on a hybrid quadrupole time-of-flight mass spectrometer. *Metabolites.* 2012;2:195–213.
12. Breslow DK, Collins SR, Bodenmiller B, Aebersold R, Simons K, Shevchenko A, et al. Orm family proteins mediate sphingolipid homeostasis. *Nature.* 2010;463:1048–53.
13. Han X. Characterization and direct quantitation of ceramide molecular species from lipid extracts of biological samples by electrospray ionization tandem mass spectrometry. *Anal Biochem.* 2002;302:199–212.
14. Merrill AH, Sullards MC, Allegood JC, Kelly S, Wang E. Sphingolipidomics: high-throughput, structure-specific, and quantitative analysis of sphingolipids by liquid chromatography tandem mass spectrometry. *Methods.* 2005;36:207–24.
15. Bielawski J, Szulc ZM, Hannun YA, Bielawska A. Simultaneous quantitative analysis of bioactive sphingolipids by high-performance liquid chromatography-tandem mass spectrometry. *Methods.* 2006;39:82–91.
16. Jiang H, Hsu F-F, Farmer MS, Peterson LR, Schaffer JE, Ory DS, et al. Development and validation of LC-MS/MS method for determination of very long acyl chain (C22:0 and C24:0) ceramides in human plasma. *Anal Bioanal Chem.* 2013;405:7357–65.
17. US Department of Health and Human Services, Food and Drug Administration, Center for Drug Evaluation and Research and Center for Veterinary Medicine (2001) Guidance for Industry: Bioanalytical method validation. <http://www.fda.gov/downloads/Drugs/Guidance/ucm070107.pdf>
18. Vaara S, Nieminen MS, Lokki M-L, Perola M, Pussinen PJ, Allonen J, et al. Cohort profile: the corogene study. *Int J Epidemiol.* 2012;41:1265–71.
19. Ann Q, Adams J. Structure determination of ceramides and neutral glycosphingolipids by collisional activation of  $[M + Li]^+$  ions. *J Am Soc Mass Spectrom.* 1992;3:260–3.
20. Hsu F-F, Turk J. Characterization of ceramides by low energy collisional-activated dissociation tandem mass spectrometry with negative-ion electrospray ionization. *J Am Soc Mass Spectrom.* 2002;13:558–70.
21. Hsu F-F, Turk J, Stewart ME, Downing DT. Structural studies on ceramides as lithiated adducts by low energy collisional-activated dissociation tandem mass spectrometry with electrospray ionization. *J Am Soc Mass Spectrom.* 2002;13:680–95.
22. Schiller J, Arnhold J, Glander HJ, Arnold K. Lipid analysis of human spermatozoa and seminal plasma by MALDI-TOF mass spectrometry and NMR spectroscopy—effects of freezing and thawing. *Chem Phys Lipids.* 2000;106:145–56.
23. Li W, Tang Y, Guo J, Shang E, Qian Y, Wang L, et al. Comparative metabolomics analysis on hematopoietic functions of herb pair Gui-Xiong by ultra-high-performance liquid chromatography coupled to quadrupole time-of-flight mass spectrometry and pattern recognition approach. *J Chromatogr A.* 2014;1346:49–56.
24. Sonomura K, Kudoh S, Sato TA, Matsuda F. Plasma lipid analysis by hydrophilic interaction liquid chromatography coupled with electrospray ionization tandem mass spectrometry. *J Sep Sci.* 2015;38:2033–7.
25. Krishnamurthy K, Dasgupta S, Bieberich E. Development and characterization of a novel anti-ceramide antibody. *J Lipid Res.* 2007;48:968–75.
26. Scherer M, Schmitz G, Liebisch G. High-throughput analysis of sphingosine 1-phosphate, sphinganine 1-phosphate, and lysophosphatidic acid in plasma samples by liquid chromatography-tandem mass spectrometry. *Clin Chem.* 2009;55:1218–22.
27. Taylor RL, Grebe SK, Singh RJ. Quantitative, highly sensitive liquid chromatography-tandem mass spectrometry method for detection of synthetic corticosteroids. *Clin Chem.* 2004;50:2345–52.
28. Gold H, Mirzaian M, Dekker N, Ferraz MJ, Lugtenburg J, Codée JDC, et al. Quantification of globotriaosylsphingosine in plasma and urine of fabry patients by stable isotope ultraperformance liquid chromatography-tandem mass spectrometry. *Clin Chem.* 2013;59:547–56.
29. Müller MJ, Volmer DA. Mass spectrometric profiling of vitamin D metabolites beyond 25-hydroxyvitamin D. *Clin Chem.* 2015;61:1033–48.
30. Ng TWK, Ooi EMM, Watts GF, Chan DC, Meikle PJ, Barrett PHR. Association of plasma ceramides and sphingomyelin with VLDL apoB-100 fractional catabolic rate before and after rosuvastatin treatment. *J Clin Endocrinol Metab.* 2015;100:2497–501.
31. Xia JY, Holland WL, Kusminski CM, Sun K, Sharma AX, Pearson MJ, et al. Targeted induction of ceramide degradation leads to improved systemic metabolism and reduced hepatic steatosis. *Cell Metab.* 2015;22:266–78.
32. Perman JC, Boström P, Lindbom M, Lidberg U, StÅhlman M, Hägg D, et al. The VLDL receptor promotes lipotoxicity and increases mortality in mice following an acute myocardial infarction. *J Clin Invest.* 2011;121:2625–40.
33. Sampaio JL, Gerl MJ, Klose C, Ejsing CS, Beug H, Simons K, et al. Membrane lipidome of an epithelial cell line. *Proc Natl Acad Sci U S A.* 2011;108:1903–7.
34. Han X, Rozen S, Boyle SH, Hellegers C, Cheng H, Burke JR, et al. Metabolomics in early Alzheimer’s disease: identification of altered plasma sphingolipidome using shotgun lipidomics. *PLoS One.* 2011;6:e21643.